Available online at www.sciencedirect.com
SCIENCE DIRECT
Diamond & Related Materials 15 (2006) 928 – 931
DIAMOND AND RELATED MATERIALS
www.elsevier.com/locate/diamond

Diamond-like carbon coatings for Ultracold Neutron applications

T. Brys [a], M. Daum [a], P. Fierlinger [a,b], A. Foelske [a], M. Gupta [a], R. Henneck [a], S. Heule [a,b,*], M. Kasprzak [a], K. Kirch [a], M. Kuzniak [a], T. Lippert [a], M. Meier [a], A. Pichlmaier [a], U. Straumann [b]

[a] *Paul Scherrer Institut (PSI), Villigen, Switzerland*
[b] *Physics Institute of the University of Zurich, Switzerland*

Available online 2 December 2005

Abstract

Diamond-like carbon (DLC) is a promising new wall coating material for use in applications with Ultracold Neutrons (UCN). It can potentially replace the toxic beryllium which has been widely used for the storage and transport of UCN.

Our aim is to produce DLC-coated neutron guide tubes of up to 1.2 m length with a Pulsed Laser Deposition (PLD) setup which is currently under construction. In order to find optimal process parameters and appropriate settings for the tube coating facility, we are carrying out a research program which includes the production and characterization of DLC films on small test samples.

The characterization of the test samples is done by Raman spectroscopy, X-ray Photoelectron Spectroscopy (XPS) and Neutron Reflectometry. We report on first results from the test samples with sp^3 fractions up to 55% and give an overview of the tube coating setup.

Keywords: Diamond-like carbon; Ultracold Neutrons; Pulsed Laser Deposition; Characterization

1. Introduction

Ultracold Neutrons (UCN) have velocities up to 8 m/s (corresponding to kinetic energies below ~300 neV) and can be described as an ideal gas with a temperature of several milli-Kelvin [1]. At these low energies their trajectories in vacuum are affected by gravitation, by magnetic fields and by the strong interaction with nuclei. In order to describe the strong interaction, a pseudo potential, called the Fermi potential, can be defined for each material. Neutrons with kinetic energy below the Fermi potential of a material are reflected under any angle of incidence. From the Fermi potential V, the critical velocity

$$v_c = (2 \cdot V / m_n)^{1/2}$$

can be calculated, where m_n is the mass of the neutron. As the UCN energy spectrum usually follows a Maxwellian, the probability for finding a neutron is proportional to its kinetic energy and it is therefore of advantage to use a material with a high Fermi potential.

On each collision with the wall the UCN has a certain probability to be absorbed or inelastically scattered, i.e. to be lost. This loss probability is proportional to the loss coefficient η, which is material-dependent. Optimal materials are therefore materials with high Fermi potential and small loss coefficient. So far, beryllium (V=252 neV) has been widely used for that purpose, but as it is highly toxic there are efforts made to replace it.

One of the most promising replacement candidates is diamond-like carbon (DLC). Pure diamond with a sp^3 fraction of 1 has a Fermi potential of 304 neV which is consequently the theoretical limit for DLC. At the same time, the theoretical loss coefficient of diamond is one of the lowest of all known materials.

For UCN applications, the materials used should not contain large amounts of hydrogen as then the UCN are immediately upscattered on hydrogen atoms. The DLC coating should therefore be produced in a process which minimizes the amount of incorporated hydrogen. This can be realised using a Physical Vapour Deposition (PVD) method such as Pulsed Laser Deposition (PLD) [2]. For UCN applications, the coating thickness should be in the range of 100 to 300 nm.

* Corresponding author. Paul Scherrer Institut, 5232 Villigen PSI, Switzerland. Tel.: +41 56 310 32 67; fax: +41 56 310 32 94.
E-mail address: stefan.heule@psi.ch (S. Heule).

0925-9635/$ - see front matter © 2005 Elsevier B.V. All rights reserved.
doi:10.1016/j.diamond.2005.10.029

Recently, the performance of DLC for UCN applications was studied in detail [3]. It was shown that DLC is comparable to beryllium with respect to loss and depolarization upon wall collisions. The DLC coatings in this study were produced by PLD [4] and by vacuum arc deposition [5].

At PSI we are presently setting up a new, high-intensity source for UCN [6]. Spallation neutrons will be produced by the impact of 600 MeV protons from the PSI proton accelerator on a lead target. These neutrons are subsequently moderated to thermal energies in a heavy water volume and further slowed down to the UCN regime by 30 l of solid deuterium. The production of UCN will be performed during 8 s in intervals of 800 s. As the typical UCN experiments have filling times longer than the production pulse, the UCN have to be stored in between two production pulses. A prototype of such a storage volume, made out of DLC-coated stainless steel foils, has been recently tested with promising results [7].

In addition to the storage volume, we will also employ DLC-coated neutron guides. In order to produce these guide tubes, we are currently setting up a PLD facility, as presented in Section 4.

2. Coating of small test samples

We used an existing PLD setup at PSI to produce flat test samples of 10×10 mm^2 and 20×20 mm^2 size. This setup is described in [8]. We investigated the influence of different process parameters on the film quality, i.e. on the film density and the corresponding sp^3 fraction. The process parameters studied were the distance between target and substrate, the coating angle, the laser fluence and the vacuum conditions during deposition.

Spectroscopically pure graphite with a density of 2.21 g/cm^3 was used as target material. Most of the DLC films were deposited on standard silicon wafers; a few samples have also been produced with stainless steel substrates, in order to check for a dependence of the film density on the substrate material.

For the production of the test samples, an excimer laser (Lambdaphysik LPX105E, KrF, 248 nm) and a Nd:YAG-laser with frequency quadrupling (266 nm) were used. The samples were produced at pressures in the range of 10^{-5}–10^{-3} Pa.

In order to study the ionic composition (see e.g. Ref. [9]) of the ablation plume emission spectra of the plume were recorded with an spectrometer (ARC SpectraDrive).

After the deposition, the thickness of the deposited DLC films was measured with a profilometer (Dektak 8000).

3. Characterization results

We have recently developed a suitable characterization procedure for our test samples by conducting a comparative study of five different characterization methods for DLC samples [10]. Following this, the DLC films were measured with Raman Spectroscopy, X-ray Photoelectron Spectroscopy (XPS) and with Cold Neutron Reflectometry (only the 20×20 mm^2 samples).

The Raman measurements were performed on a Dilor LabRam spectrometer. The excitation light source was a HeNe laser at 632.8 nm with a power of 25 mW. A grating with 1800 l/mm was used. Following the procedure described in Ref. [10], we used a calibration curve to calculate the sp^3 fraction and the film density from the width of the Raman G band. The original calibration curve was extended to correctly evaluate the lower film densities of our test samples (compared to the reference samples used in [10]). The Raman G band and D band were both fitted with Gaussians.

Part of the samples was also measured with XPS. The measurements were performed on an ESCALAB 220i XL spectrometer using an Al Kα monochromatic X-ray source. For the fit parameters in the analysis, the same constraints as in [10] were used.

The samples with 20×20 mm^2 size were additionally measured with Cold Neutron Reflectometry, which is not a commonly used method to characterize DLC films but very suitable for DLC used in UCN applications. Cold neutrons have velocities above those of UCN, up to 1000 m/s. If the velocity component normal to the reflecting surface is smaller than the critical velocity, the neutron is reflected. This is the case for cold neutrons under glancing incidence. The reflectivity is measured as a function of the neutron velocity and the angle of incidence. The critical velocity can then be derived from the reflectivity curve.

All three methods show consistent results for the investigated test samples. Diamond fractions in the range of 20–55% were measured, depending on the different production process parameters used.

The dependence of the sp^3 fraction on the distance between target and substrate was investigated first. The results from a sample series, in which all process parameters except for the target–substrate distance were fixed, showed that the film density is constant for distances in the range of 2.5 cm–5.5 cm. However, as this series consisted of films with a low sp^3 fraction, we will repeat the series, choosing process parameters that will lead generally to a higher diamond fraction.

The second parameter studied was the laser fluence on the target. This was achieved by changing the voltage in case of the excimer laser and by using an attenuator with the Nd:YAG laser. Alternatively the laser fluence can also be changed via the position of the focussing lens, changing the spot size on the target. In general, we measured higher sp^3 fractions for higher laser fluences. Fig. 1 shows the XPS spectra of four samples, deposited with different laser fluences while all the other process parameters (distance between target and silicon substrate, pressure, laser wavelength) were kept constant. The values for the sp^3 fraction derived from the XPS spectra, following Ref. [11] and using the XPSPeak software [12], range from 22% for $1.3 \cdot 10^8$ W/cm^2 to 34% for $2.7 \cdot 10^8$ W/cm^2, which is close to the maximum laser fluence that was achieved and which may be marginal for high-density DLC films [13]. However, for our target the highest laser power in connection with an optimally focussed beam led to an undesired deposition of graphite particulates.

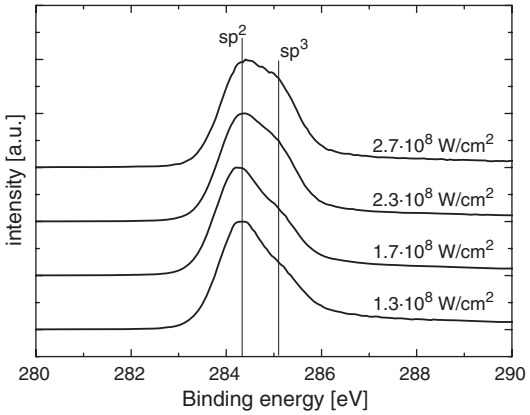

Fig. 1. XPS spectra of four samples deposited with different laser fluences. An increase of the sp^3 fraction at increasing laser fluence was found. The values for the sp^3 fraction range from 22% for the lowest laser fluence to 34% for the highest laser fluence. The sp^2 and sp^3 binding energies are indicated by the vertical lines at 284.4 eV and 285.2 eV. The increased sp^3 fraction for higher laser fluence is indicated by the hump at binding energies around 285 eV.

The third process parameter studied was the pressure in the deposition chamber during the laser ablation process. The lowest pressure that could be reached with the chamber was about $3\cdot10^{-5}$ Pa. Samples were deposited at pressures up to $3\cdot10^{-3}$ Pa. The deposition rates were found to be similar for the different pressures used, e.g. about 0.2 nm/s for both $5\cdot10^{-5}$ Pa and $1.5\cdot10^{-3}$ Pa (target–substrate distance 4 cm, excimer laser).

We also investigated the film density as a function of the deposition angle α, as shown in Fig. 2. The plume (item 4 in the insert of Fig. 2) was observed to stand normal to the target surface. We adjusted the laser beam (item 1) to hit a spot on the cylindrical target (item 2) such that the resulting plume was directed to the substrate (item 5). The substrate with 20×20 mm^2 size was set to a distance of about 25 mm from the target surface in order to cover a large solid angle around the target spot (item 3). A series of points on the diagonal from one edge to the centre of the sample was measured with Raman and XPS. The resulting sp^3 fractions of

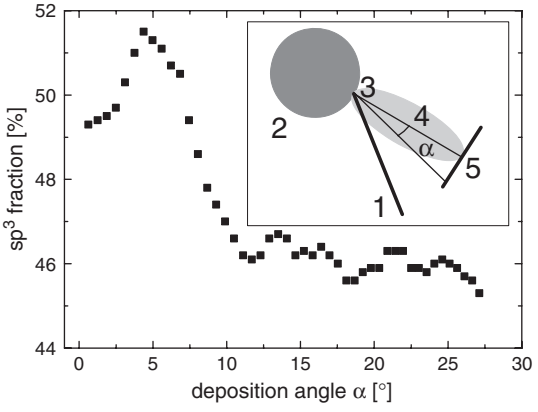

Fig. 2. Diamond fraction as a function of the deposition angle α, measured with XPS. Insert: (1): laser beam, (2): target, (3): target spot, (4): plume, (5): substrate.

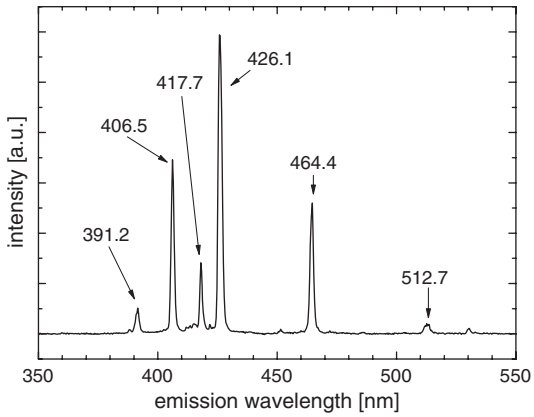

Fig. 3. Emission spectrum for PLD of DLC at 266 nm wavelength (Nd:YAG laser). For details, see text.

the XPS measurements are plotted in Fig. 2. The highest values for the sp^3 fraction were reached for positions slightly off centre. For $\alpha\leq5°$, the sp^3 fraction is up to 5% higher than for larger deposition angles.

As our aim is to deposit DLC not only on silicon, but also on different materials as stainless steel, aluminium or quartz, we compared the resulting sp^3 fraction for fixed process parameters on silicon and stainless steel substrates. With XPS and Raman spectroscopy, we found no significant difference in the sp^3 fraction between the two substrate materials, e.g. (33.8 ± 2.0)% on stainless steel vs. (32.8 ± 0.4)% on silicon, both measured with XPS and deposited at a laser fluence of approximately $2\cdot10^8$ W/cm^2 and 248 nm wavelength. The target to substrate distance was about 3 cm and the pressure during deposition $2\cdot10^{-3}$ Pa. Nearly identical film thickness of 100 nm was achieved for the two samples.

Fig. 3 shows an emission spectrum recorded during a DLC deposition at 266 nm laser wavelength. The lines at 391.2, 426.1 and 512.7 nm were identified to originate from C^+ ions and those at 406.5, 417.7 and 464.4 nm from C^{2+} ions (see e.g. [14]). A systematic analysis of the emission spectra, especially a comparison of the line intensities with the sp^3 fraction of the corresponding samples, was started and is still ongoing.

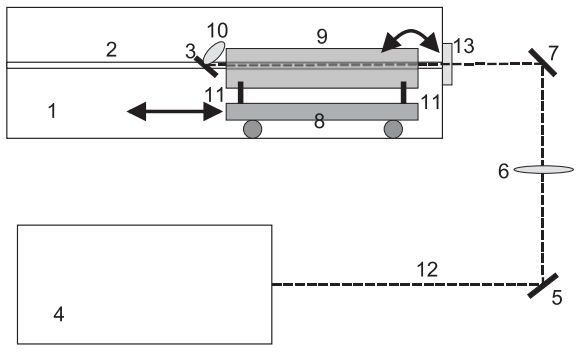

Fig. 4. Schematic overview of the tube coating PLD facility. (1): Vacuum chamber, (2): target tube, (3): target, (4): excimer laser, (5): fixed mirror, (6): focussing lens, (7): kinematic mirror, (8): trolley, (9): substrate tube, (10): ablation plume, (11): wheels for substrate rotation, (12): laser beam.

4. Tube coating setup

As mentioned in the introduction, we intend to coat the insides of tubes. A schematic diagram of the setup is shown in Fig. 4. It consists of a 3-m-long vacuum chamber (item 1 in Fig. 4) with an inner diameter of 40 cm. The target tube (item 2) of the same length is mounted slightly off-axis several centimetres above the central axis of the vacuum tube. A flat target (item 3), made out of highly pure graphite or glassy carbon, some square centimetres in size, is fixed in the middle of the target tube. The laser beam (item 12), coming from an excimer laser (Lambdaphysik LPX-301, item 4) enters the vacuum tube through a quartz window (item 13). The target tube has a radial opening at the target location.

The incident laser beam is scanned over the target by a fast steering mirror system located just outside the vacuum tube (item 7). The laser beam is focused by a quartz lens (item 6) with a focal length of about 1.5 m.

The substrate, a tube of up to 1.2 m length and diameter of 60–250 mm, is sitting on two sets of wheels (item 11) which are mounted on the top of a trolley (item 8). This allows moving the tube over the target while simultaneously rotating it around the target tube.

In a first step, we will assemble only part of the setup without the moving/rotating mechanics. With this setup, we will perform focus tests and first coating tests on small samples comparable to the test samples described in Section 2. Focus tests are crucial as the major disadvantage of an excimer laser is its large divergence (up to 3 mrad) which leads to large minimal spot size (in the order of 1 mm^2) when focussed over large distances ($f \geq 1$ m). A large focal point would lead to only moderate laser power densities, possibly too low to produce DLC films with high density. Therefore, our excimer laser is equipped with so-called unstable optics which nominally reduces the divergence to 0.4×0.4 $mrad^2$, although the laser intensity drops to 50%. The resulting gain factor for focal lengths around 1.5 m can be up to 20.

5. Conclusions

We have produced test samples with sp^3 fractions up to 55% with a Nd:YAG laser at 266 nm and up to 45% with an excimer laser at 248 nm. No significant dependence on the target–substrate distance was observed over the available range of 2.5 to 5.5 cm. We found higher laser fluences to produce DLC films with higher sp^3 fractions. However, at very high laser fluences the sp^3 fraction was limited by the incorporation of ejected graphite particulates. The highest value of the sp^3 fraction was found for deposition at angles close to the normal of the substrate surface.

For the new setup, we shall concentrate on excimer lasers as there seems more potential for improved ablation performance than for Nd:YAG lasers, mainly based on the achievable power density and the shorter wavelength. Furthermore, due to the smaller spot size of the laser beam on the target, the deposition rates with Nd:YAG lasers are significantly lower than for excimer lasers and would result in unacceptably long deposition times for the tube setup.

We shall employ a more powerful excimer laser than the one used up to now and as it is known that going to shorter wavelengths increases the sp^3 fraction [15], we will change from 248 nm (KrF) to 193 nm (ArF). The addition of these improvements will provide laser power densities, which should be sufficient to produce DLC with a density approaching that of pure diamond [13].

Acknowledgement

This work was performed at the Paul Scherrer Institut, Villigen. We appreciate the valuable discussions with T. Dumont, T. Gutberlet, L. Hardwick, R. Koetz, G. Kopitkovas, C.-F. Meyer, M. Montenegro and L. Urech. This work is supported by the Swiss National Science Foundation (grant 200021-105400).

References

[1] V. Ignatovich, The Physics of Ultracold Neutrons, Oxford University Press, USA, 1990.
[2] A.A. Voevodin, M.S. Donley, Surface and Coatings Technology 82 (1996) 199.
[3] F. Atchison, T. Brys, M. Daum, P. Geltenbort, R. Henneck, S. Heule, M. Kasprzak, K. Kirch, A. Pichlmaier, C. Plonka, U. Straumann, C. Wermelinger, Physics Letters B 625 (2005) 19.
[4] M. Makela, PhD thesis, advised by B. Vogelaar, Virginia Polytechnic Institute and State University, 2005.
[5] H.-J. Scheibe, B. Schultrich, H. Ziegele, P. Siemroth, IEEE Transactions on Plasma Science 25 (1997) 685.
[6] A. Fomin et al., PSI-Report TM-00-14-01 (2000).
[7] B. Blau, T. Brys, P. Fierlinger, P. Geltenbort, R. Henneck, S. Heule, M. Kasprzak, K. Kirch, K. Kohlik, M. Meier, A. Pichlmaier, G. Zsigmond, PSI Annual Report 2004, Part I.
[8] P.R. Willmott, J.R. Huber, Reviews of Modern Physics 72 (2000) 315.
[9] R. Diamant, E. Jimenez, E. Haro-Poniatowski, L. Ponce, M. Fernandez-Guasti, J.C. Alonso, Diamond and Related Materials 8 (1999) 1277.
[10] F. Atchison, T. Brys, M. Daum, P. Fierlinger, A. Foelske, M. Gupta, R. Henneck, S. Heule, M. Kasprzak, K. Kirch, R. Koetz, M. Kuzniak, T. Lippert, C.-F. Meyer, F. Nolting, A. Pichlmaier, D. Schneider, B. Schultrich, P. Siemroth, U. Straumann (in press).
[11] P. Merel, M. Tabbal, M. Chaker, S. Moisa, J. Margot, Applied Surface Science 136 (1998) 105.
[12] XPS Peak, written by R. Kwok, download at http://www.phy.cuhk.edu.hk/~surface/XPSPEAK/.
[13] D.L. Pappas, K.L. Saenger, J. Bruley, W. Krakow, J.J. Cuomo, T. Gu, R.W. Collins, Journal of Applied Physics 71 (1992) 5675.
[14] A.M. Keszler, L. Nemes, Journal of Molecular Structure 695–696 (2004) 211.
[15] K. Yamamoto, Y. Koga, S. Fujiwara, F. Kokai, R.B. Heimann, Applied Physics. A 66 (1998) 115.